



**NIST Grant/Contractor Report
NIST GCR 22-036**

Research on Estimating Peak Water Demands and Measuring Pressure Losses in Premise Plumbing Systems

Steven Buchberger
Tao Li
Toritseju Omaghomi
University of Cincinnati

Gary Klein
Gary Klein Associates

This publication is available free of charge from:
<https://doi.org/10.6028/NIST.GCR.22-036>

**NIST Grant/Contractor Report
NIST GCR 22-036**

Research on Estimating Peak Water Demands and Measuring Pressure Losses in Premise Plumbing Systems

Prepared for
*U.S. Department of Commerce
Engineering Laboratory
National Institute of Standards and Technology
Gaithersburg, MD 20899*

By
Steven Buchberger
Tao Li
Toritseju Omaghome
University of Cincinnati

Gary Klein
Gary Klein Associates

This publication is available free of charge from:
<https://doi.org/10.6028/NIST.GCR.22-036>

January 2023



U.S. Department of Commerce
Gina M. Raimondo, Secretary

National Institute of Standards and Technology
Laurie E. Locascio, NIST Director and Under Secretary of Commerce for Standards and Technology

Disclaimer

This publication was produced as part of cooperative agreement 70NANB21H014 with the National Institute of Standards and Technology. The contents of this publication do not necessarily reflect the views or policies of the National Institute of Standards and Technology or the US Government.

Certain commercial entities, equipment, or materials may be identified in this document in order to describe an experimental procedure or concept adequately. Such identification is not intended to imply recommendation or endorsement by NIST, nor is it intended to imply that the entities, materials, or equipment are necessarily the best available for the purpose.

NIST Technical Series Policies

[Copyright, Fair Use, and Licensing Statements](#)

[NIST Technical Series Publication Identifier Syntax](#)

How to Cite this NIST Technical Series Publication

Buchberger S, Li T, Omaghomi T, Klein G (2023) Research on Estimating Peak Water Demands and Measuring Pressure Losses in Premise Plumbing Systems. (National Institute of Standards and Technology, Gaithersburg, MD), NIST Grant/Contractor Report (GCR) NIST GCR 22-036.
<https://doi.org/10.6028/NIST.GCR.22-036>

Abstract

A protocol is described for conducting a survey to monitor instantaneous peak water use in non-residential buildings using a new wireless sensor network technology. The protocol enables compilation of a nationally representative water use database from which key parameters can be extracted and then applied to calibrate the Water Demand Calculator for predicting instantaneous peak water demand in non-residential buildings. In addition, the report summarizes a conceptual plan for a laboratory facility for conducting experiments to determine flow pressure loss across fittings and other hydraulic appurtenances commonly found in modern premise plumbing systems.

Keywords

Commercial Buildings, Peak Water Demand, Pressure Loss, Wireless Sensor, Water Demand Calculator.

Table of Contents

Abstract	i
List of Tables	iii
List of Figures	iii
List of Notation	iv
Glossary of Acronyms/Abbreviations	v
1. Introduction	1
2. Research Objectives	4
3. Task 1: Commercial Building Survey	5
3.1. Types of Commercial and Institutional (CI) buildings	5
3.2. Sample Size Determination	6
3.3. Probability of Fixture Use.....	8
3.3.1. Probability Calculation	8
3.3.2. Simulation Exercise	10
3.4. Sampling Methods	12
3.4.1. Probability Sampling Methods.....	12
3.4.2. Non-Probability Sampling Methods.....	13
4. Task 2: Wireless Sensor Network	15
4.1. Overall System.....	15
4.2. Sensor Module Design.....	15
4.2.1. Overall Design of Sensor Module	15
4.2.2. Sensor Modality 1	16
4.2.3. Sensor Modality 2.....	22
4.3. Sensor Network Implementation.....	27
4.3.1. Overview	27
4.3.2. Zigbee Wireless Network Configuration.....	27
4.3.3. System Software Architecture	28
4.3.4. Data Frame Definition.....	29
5. Task 3: Pressure Loss in PPS	30
6. Summary and Recommendations	34
7. References	35
Appendix A: Survey of plumbing industry at 2021 ASPE Technical Symposium	37

List of Tables

Table 1. Classifications and examples of CI buildings.....	5
Table 2. Hypothetical sampling plan for several categories of CI buildings	14
Table 3. Comparison of candidate methods for signal strength indicator functions.....	17
Table 4. Different audio recordings and their test results.	19

List of Figures

Fig. 1. Input template for Water Demand Calculator.....	3
Fig. 2. Graphical solutions to Equation (1)	8
Fig. 3. Definition sketch for queueing theory applied to plumbing fixture use.....	11
Fig. 4. Dimensionless $(p) (\rho)$ diagram; probability plateau occurs at congestion.....	12
Fig. 5. System concept design.	15
Fig. 6. Sensor module diagram.	16
Fig. 7. Functional block diagram for device configuration for Stage 1 testing.....	19
Fig. 8. SM1 microphone integration.	21
Fig. 9. Stage 1 test Setup.	21
Fig. 10. Calorimetric thermal flow sensing method.	22
Fig. 11. Assembled PCB: top side (top), bottom side (bottom).	23
Fig. 12. Holder design.....	24
Fig. 13. Assembled test PCB for SM2 on PCB holder.....	24
Fig. 14. Schematic of test setup design (top) and photo of implemented setup (bottom)....	25
Fig. 15. Temperature response graph.....	26
Fig. 16. Zigbee network topology.	28
Fig. 17. System software architecture.	29
Fig. 18. Custom data frame used to report data from end device to gateway.	30
Fig. 19. Pressure testing lab in Southern California.....	31
Fig. 20. Pressure testing lab in Arcata, California.....	32
Fig. 21. Target flow rates for ½ -inch nominal pipe.....	32
Fig. 22. Pressure loss through ½-inch copper elbows and tees.....	33
Fig. 23. Pressure loss through ½-inch PEX elbows, tees, and couplings.	34

List of Notation

Symbol	Meaning	Unit
a	Fixture activation factor	Dimensionless
e	Percentage margin of error	Dimensionless
k	Number of identical fixtures in a restroom	-
m	Number of water use events at fixtures	-
N	Number of people departing a restroom	-
n_0	Sample Size	-
p	Probability of water flowing at a fixture	Dimensionless
q	Fixture flowrate	Liters (Gallons) per minute
t	Duration of flow at a fixture	Minutes, Seconds
t_m	Duration of flow for all m water use events	Minutes, Seconds
T	Duration of fixture observation	Minutes, Seconds
T_0	Duration when a fixture is occupied	Minutes, Seconds
V	Volume of flow per pulse	Liters (Gallons)
z	Standard score in the normal distribution table	-
(Greek letters)		
λ	Arrival rate	Per minute
τ	Duration of flow at fixture per pulse	Minutes, Seconds
μ	Service rate	Per minute
ρ	Utilization factor	Dimensionless

Glossary of Acronyms/Abbreviations

ADC	Analog-Digital Converter
ARM	Advanced RISC (<i>Reduced Instruction Set Computer</i>) Machine
ASPE	American Society of Plumbing Engineers
AWWA	American Water Works Association
BLE	Bluetooth Low Energy
CI	Commercial and Institutional
CBECS	Commercial Buildings Energy Consumption Survey
CPVC	Chlorinated Polyvinyl Chloride
EIA	Energy Information Administration
EPAct92	Energy Policy Act of 1992
FoM	Figure of Merit
GPM	Gallons per Minute
IAPMO	International Association of Plumbing and Mechanical Officials
IIR	Infinite Impulse Response
MEMS	Micro Electromechanical Systems
MCU	Microprocessor Unit
MQTT	MQ Telemetry Transport (open messaging protocol)
NBS	National Bureau of Standards
NIST	National Institute of Standards and Technology
PCB	Printed Circuit Board
PEX	Cross-linked Polyethylene Pipe
PP	Polypropylene Pipe
PVC	Polyvinyl Chloride Pipe
RMS	Root Mean Square
SM(k)	Sensor Modality (k)
SMA	Simple Moving Average
SMD	Surface Mount Device
SNR	Signal to Noise Ratio
UART	Universal Asynchronous Receiver-Transmitter
UC	University of Cincinnati
UPC	Uniform Plumbing Code
WDC	Water Demand Calculator
WQA	Water Quality Association

1. Introduction

Instantaneous peak water demand is an important consideration when designing a new building. The peak water demand affects the scale and cost of the entire premise plumbing system, including meter size, heater capacity, pipe diameters, valves, and other related hydraulic appurtenances. Determining the peak water demand is challenging because water use in a building is unpredictable. The diurnal pattern of water use never repeats exactly, and, as a consequence, the magnitude of the peak demand varies randomly from day to day.

This problem was first investigated nearly 100 years ago by Dr. Roy Hunter, a research physicist at the National Bureau of Standards. Recognizing that water use is a random process, Hunter applied probability principles to predict peak water demand based on the total number of fixtures in a building and on the flow drawn when a fixture is operated. The peak demand determines the size of the service line and many other features of the premise plumbing system.

Hunter's crowning achievement was the development of a design graph known as "Hunter's Curve", giving the 99th percentile water demand versus total fixture units for any combination of indoor end uses (Hunter 1940). Hunter did not attempt to predict the absolute maximum possible water demand. Instead, he defined a threshold for design so that there is only a 1 % chance that the actual peak period demand will exceed the load estimated from his curve.

Hunter's iconic curve is an ingenious blend of theoretical rigor and practical simplicity. It quickly became the basis for plumbing codes in the United States and across the globe (Buchberger *et al.*, 2012). Hunter's work established the standard for satisfactory service of building water supply systems. The problem, however, is that Hunter's curve is frozen in time; it is a snapshot of peak indoor water use in 1940.

In recent years, a growing consensus has emerged among practicing engineers that Hunter's curve leads to overdesign of the premise plumbing system in new buildings (USNCCIB 1974; Banazzi *et al.* 1976; Steele 1982). There are a couple of reasons for this. First, Hunter's assumption of congested service (*i.e.*, users queue at fixtures) often does not hold. Second, flow rates based on plumbing fixtures from the 1930s do not apply to the new generation of water-conserving fixtures, especially those imposed by the passage of the 1992 Energy Policy Act and subsequent green plumbing codes.

There have been many attempts to salvage Hunter's curve by tweaking fixture-unit values for contemporary end-use applications. Often these modifications reflect engineering judgment rather than observable data. These ad hoc adjustments have led to discrepancies among fixture-unit values posted in various plumbing codes (Cole 2012).

In 2011, the International Association of Plumbing and Mechanical Officials (IAPMO), the American Society of Plumbing Engineers (ASPE), and the University of Cincinnati (UC), in

collaboration with the Water Quality Association (WQA), convened a task group to review methods for estimating peak demands in buildings fitted with water-conserving fixtures.

The task group acquired a large database of high-resolution indoor water use measurements taken between 1996 and 2011 at nearly 1100 single-family homes in 62 cities across the United States (Buchberger *et al.*, 2017). Because the dataset provided statistics for residential end use only, the scope of work was narrowed to single and multi-family residential dwellings. Residential indoor fixtures considered in the database were bathtubs, showers, dishwashers, clothes washers, faucets, and toilets.

The task group was charged with developing a probability model to predict the peak water demand for single- and multi-family dwellings having water-conserving plumbing fixtures. In other words, the goal was to bring Hunter's curve into the 21st century. Not surprisingly, analysis of the modern residential database led to several significant changes in the parameters of the binomial probability model that underpins Hunter's method. Most notably, for tank toilets, the peak hour probability of fixture use dropped from 20 % to 1 %, and the fixture flow rate decreased from 15 Liters Per Minute (LPM) to 11 LPM (4 Gallons Per Minute [GPM] to 3 GPM) (Omaghomi *et al.*, 2020). A complete listing of all recalibrated parameter values for water-conserving residential fixtures is available in the summary report (Buchberger *et al.*, 2017).

Rather than create a new design curve that essentially would be a snapshot of peak water use in 2020, the task group opted to employ a digital-age resource. Keeping with the spirit of Hunter's probabilistic approach, a set of three algorithms was coded into a user-friendly spreadsheet called the Water Demand Calculator (WDC). The user simply provides the itemized fixture count for their residential building. Then, armed with information about the probability of fixture use and flow of an operating fixture (the p and q values, respectively), the WDC computes the 99th percentile of the peak period water demand. The WDC program is available at no charge from the IAPMO website. Figure 1 shows the WDC input template and computed results for a multi-family building with ten apartments.

For single-family homes, where the total fixture count is generally under 30, the WDC uses exhaustive enumeration (ExEn) to delineate all possible water use combinations. While offering an exact solution, ExEn carries a high computational burden. For instance, in a home with 15 fixtures, ExEn involves 2^{15} or 32 768 calculations. For large residential buildings with hundreds of fixtures, ExEn is intractable. In this case, the WDC estimates the 99th percentile of the water demand using the normal approximation to the Poisson-binomial distribution, as first proposed by ASPE engineer Robert Wistort (1994). Between these household extremes, the WDC uses a new modified Wistort method to predict peak demands in the transition region from single-family homes to large residential buildings. Recently, a convolution-based algorithm suggested by Herbert (2020) has been investigated and coded into the WDC as a computational option for buildings with fixture counts under 40. Preliminary testing suggests that the convolution approach can offer

markedly improved performance (*i.e.*, reduced run times) compared to the existing exhaustive enumeration scheme.

Extensive beta testing of the WDC at several large residential locations across the United States and Australia has yielded very reasonable results. Based on this encouraging performance, the WDC has been incorporated into Appendix M of the Uniform Plumbing Code (IAPMO 2018 and 2021). With the impending release of the fourth edition of the M22 Manual of Water Supply Practice, the WDC will be endorsed by AWWA as the preferred method for estimating peak indoor water demands in all residential buildings.

Like Hunter’s seminal work from 1940, the theoretical basis for the WDC has a rock-solid foundation. With proof of concept clearly demonstrated, the framework for the WDC is poised to serve as a design aid for estimating peak demands in non-residential buildings. To extend the WDC to the non-residential sector, one major hurdle remains: there is a need to assemble and analyze a national database of water use measurements from buildings in the non-residential sector, as outlined in the recent NIST report on research needs for premise plumbing systems (Persily *et al.*, 2020). This critical step is essential to estimate values for the probability of fixture use, the elusive “*p*-values” that lie at the heart of Hunter’s curve and the WDC.

Water Demand Calculator (WDC v2.0)

PROJECT NAME : Total Number of Apartments in the Building → 10
 Click for Drop-down Menu → Total Apartments in this Calculation → 8 Wednesday, June 03, 2020
11:01 PM

FIXTURE GROUPS	FIXTURE	ENTER TOTAL NUMBER OF FIXTURES	PROBABILITY OF USE (%)	ENTER FIXTURE FLOW RATE (GPM)	MAXIMUM RECOMMENDED FIXTURE FLOW RATE (GPM)
Bathroom Fixtures	1 Bathtub (no Shower)	0	0.71	5.5	5.5
	2 Bidet	0	0.65	2.0	2.0
	3 Combination Bath/Shower	16	2.83	5.5	5.5
	4 Faucet, Lavatory	32	1.61	1.5	1.5
	5 Shower, per head (no Bathtub)	16	1.98	2.0	2.0
	6 Water Closet, 1.28 GPF Gravity Tank	32	0.65	3.0	3.0
Kitchen Fixtures	7 Dishwasher	8	0.41	1.3	1.3
	8 Faucet, Kitchen Sink	8	1.61	2.2	2.2
Laundry Room Fixtures	9 Clothes Washer	8	2.80	3.5	3.5
	10 Faucet, Laundry	4	1.61	2.0	2.0
Bar/Prep Fixtures	11 Faucet, Bar Sink	0	1.61	1.5	1.5
Other Fixtures	12 Fixture 1	4	1.50	5.5	6.0
	13 Fixture 2	0	0.00	0.0	6.0
	14 Fixture 3	0	0.00	0.0	6.0

COMPUTED RESULTS FOR PEAK PERIOD CONDITIONS

Total No. of Fixtures in Calculation
n = 128

99th Percentile Demand Flow
Q = 18.8 GPM

Hunter Number
H[n,p] = 2.00

Stagnation Probability
Pr[Zero Demand] = 13%

↓ Select Units for Water Demand ↓

Fig. 1. Input template for Water Demand Calculator

2. Research Objectives

The current version of WDC is limited to residential buildings because the data used to estimate the fixture use parameters came solely from the residential sector. There are approximately six million commercial buildings across the US (US EIA 2020), and they come in a wide variety of occupancies and sizes. There is a need to estimate the fixture parameters for the non-residential buildings in the US so that the WDC can be extended to commercial and institutional buildings.

This research project had three main objectives:

Objective 1 – Commercial Building Survey: Develop a plan to identify a representative regional or national cross-section of buildings from the commercial and institutional (CI) sector for the purpose of monitoring their water consumption, with a particular focus on gathering fixture use data during the period of peak instantaneous indoor water demand. This task identifies the various categories and types of CI buildings, including determining the sample size for each fixture in each building. Provide algorithm(s) to analyze the water use database and extract estimates of the peak hour probability of fixture use which, in turn, will extend the functionality of the public domain WDC to the commercial building sector.

Objective 2 – Wireless Sensor Network: Develop and test a novel, low-cost, battery-powered, miniature wireless sensor module for non-invasive detection of flow through pipes in premise plumbing systems. When deployed in a typical building (*e.g.*, commercial, institutional, residential, *etc.*), the modules will form a wireless sensor network to accurately monitor the incidence and patterns of water usage at various fixtures. Binary signals from these sensors will populate the database that will ultimately yield estimates of the peak period probabilities of fixture use (a key element of the first objective).

Objective 3 – Experimental Hydraulics Lab: Develop conceptual plans for a wet lab designed to investigate pressure loss across fittings and other hydraulic appurtenances commonly found in modern premise plumbing systems. The plans will include a description of the physical plant and an overview of some standard experimental methods for investigating the hydraulic performance of premise plumbing systems.

3. Task 1: Commercial Building Survey

There are four key research questions to be answered in task 1.

1. What are the types of commercial and institutional buildings to be sampled?
2. What is the sample size needed for a representative database?
3. Where can these buildings be sampled?
4. What sampling method is the most appropriate for the study?

These research questions are addressed in this section.

3.1. Types of Commercial and Institutional (CI) buildings

There is a wide range of CI buildings, varying in size and function. Some of the CI facilities listed in Table 1 are classified according to their primary activities: business, commerce, or other functions carried out within each building (Lewis 2019, US EIA 2018).

Table 1. Classifications and examples of CI buildings

Classification	Examples
Healthcare	Hospitals (inpatient/outpatient), clinics, rehabilitation centers
Offices	General office space, professional office, or administrative offices
Education	Elementary, primary, and tertiary or vocational education
Food sale	Grocery and convenience stores
Food services	Fast food, restaurants, bars, and catering service
Lodging	Hotels, motels, inn, dormitory, short term non-residential accommodations
Retail	All non-food-related retail spaces, strips, and enclosed malls
Public assembly	Community halls, convention centers, gymnasiums, museums, cinemas, sports arenas, library
Public order	Police and fire stations, correctional facilities
Religious worship	Chapels, churches, mosques, synagogues, and temples
Services	Repair shop, laundromat, salons, post office, carwash, etc.
Warehouse and storage	Rental storage units
Other buildings	Datacenter, airport hangar, laboratory, public restroom

The Commercial Buildings Energy Consumption Survey (EIA CBECS 2018) estimated there are about 5.9 million CI buildings across the US. This CI building stock contained 9 billion m² (97 billion sq feet) of floor area. This estimate reflects 6 % and 11 % increases by count and floor area, respectively, compared to the previous CBECS conducted in 2012 (US EIA 2020).

The CI buildings in the CBECS survey are dispersed from the east coast to the west coast across nine climatic regions, most of which experience significant seasonal variation in

local weather. Outside temperature, precipitation, humidity, windspeed and other weather processes exert a major influence on energy demand in buildings. Hence, from an energy perspective, it is vital to survey buildings from a wide range of geographic and climactic conditions to accurately characterize building energy consumption on a national scale.

Indoor water use is a different story. We hypothesize that *indoor* water consumption is not particularly sensitive to climate or geography in the US. That is to say, indoor water use at a school or hospital or office in Virginia is similar to indoor use at a school or hospital or office in Arkansas or Arizona or Alaska.

Clearly, outdoor water use (*e.g.*, irrigation) could vary dramatically from State to State. This study is not concerned with outdoor water use. Inside the building, we posit that the frequency or probability of water fixture use is quite similar from place to place. Indoor water use is driven by similar activities such as cleaning, cooking, washing, flushing, *etc.* Irrespective of the region, we hypothesize that these fixture operations have the same water use capacity and frequency per function. For instance, a 6 L (1.6 gallon) flush tank in California is used as often as the same 6 L (1.6 gallon) flush tank in Ohio. This is a testable hypothesis with profound implications. If confirmed, it implies that a representative national survey of indoor water use for CI buildings may be conveniently confined and completely conducted within any local region in the US.

3.2. Sample Size Determination

A representative sample of a population is a subset that reflects the characteristics of the larger group. Factors that determine the representative sample size include the population size, the allowable margin of error or level of precision, the level of confidence or risk, and the degree of variability in the attributes being measured (Israel, 2013). For this study of water use in CI buildings, the attribute of interest is the probability that water is flowing at a fixture during the peak period (fixture *p*-value). The sample size is the number of individual fixtures to be monitored. The amount of time needed to sample at each fixture is an important consideration that will be addressed in the phase 2 final report.

The level of precision (margin of error), expressed in percentage points, is the range in which the true value of the population is estimated to be. The confidence or risk level is based on the Central Limit Theorem and repeated sampling, that the samples are distributed normally about the true population value. The sum of the confidence level and the risk level equals 100. For example, if the fixture *p*-values follow a normal distribution, then approximately 95 % of the sample values will fall within two standard deviations of the population mean value. A 95 % confidence level implies there is a 5 % risk that the sample values are not within two standard deviations of the population mean value. The risk level increases as the confidence level decreases and vice versa.

The degree of variability in the attributes being measured refers to the distribution of attributes in the population. The more homogeneous a population, the smaller the sample

size required; conversely, a heterogeneous population requires a larger sample size to represent the population in similar proportions to its heterogeneous characteristics. Assuming a very large population is to be sampled, the following expression from Cochran (1977) can be used to find the sample size (number of fixtures) needed to estimate a proportion \hat{p} , the average fraction of the total fixture count that are flowing water simultaneously during the peak period,

$$n_o = \frac{z_{1-\frac{\alpha}{2}}^2 \hat{p}(1-\hat{p})}{e^2} \quad (1)$$

In Eq. 1, n_o is the required sample size (number of individual fixtures), α is the allowable risk level, $1-\alpha$ is the desired confidence level (typically, 90 %, 95 %, 99 %), $z_{1-\frac{\alpha}{2}}$ is the value of the standard normal deviate with cumulative probability $1-\alpha/2$, e is the desired level of precision (margin of error), and \hat{p} is the estimated average proportion of fixtures that are flowing water simultaneously during the peak period. Note that \hat{p} can also be interpreted as the proportion of time water is flowing at an individual fixture during the period of peak water use (*i.e.*, the fixture p -value).

Equation (1) has two unknowns, n_o on the left and \hat{p} on the right. Therefore, an iterative process may be required to reach a solution. To proceed, select a starting fixture p -value, then calculate the initial estimate for the required sample size. Collect and analyze data from the initial sample to obtain an updated fixture p -value. Use the updated p -value to calculate a refined estimate of the required sample size. Repeat this iterative process until the estimates for the sample size and/or the fixture p -values converge. It is expected that the results will converge rapidly, within a few iterations. A convenient starting reference point for fixture p -values are those tabulated in the 2017 IAPMO report for peak water demand in residential buildings.

To illustrate, assume a fixture p -value of 10 % with an allowable margin of error $\alpha = 5$ %. The confidence interval is $1-\alpha = 95$ % and the corresponding standard normal deviate, $z_{0.975} = 1.96$. Then from Eq. 1, the number of fixtures to be sampled (monitored) is

$$n_o = \frac{1.96^2 \times 0.10 \times (1-0.10)}{0.05^2} = 139 \quad (2)$$

Other solutions for Eq. 1 are plotted in Figure 2 which shows the sample size necessary for a range of \hat{p} values at a 95 % confidence interval, highlighting the region where the margin of error does not exceed 10 %.

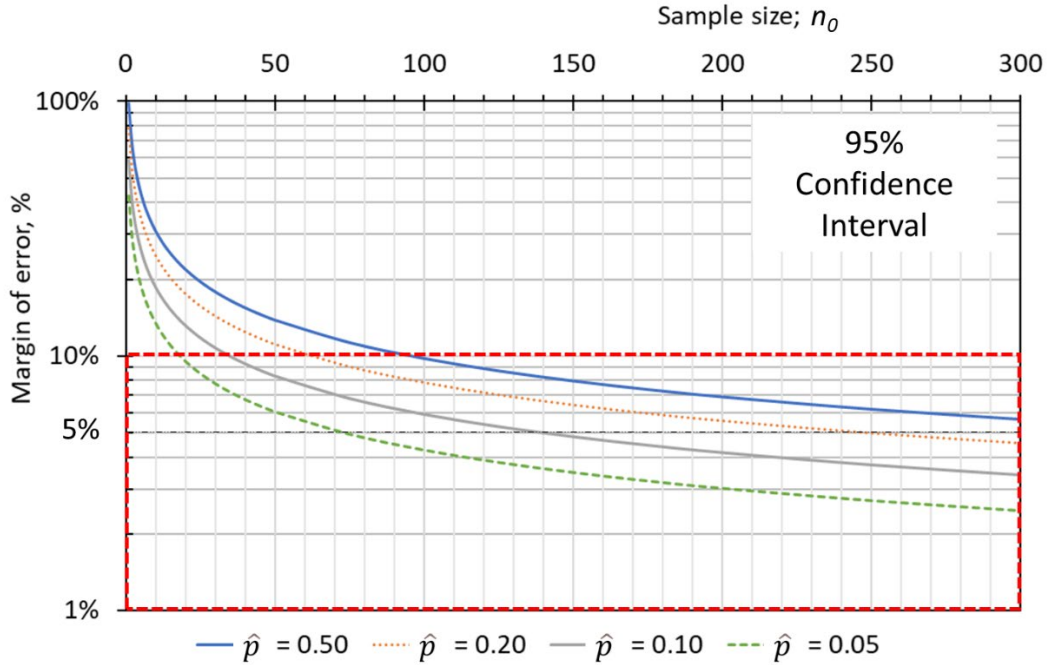


Fig. 2. Graphical solutions to Equation (1).

It might be necessary to select a sample size for a combination of precision, level of confidence, and variability justified by the resources available to sample the population. The sample size is often increased by 10 % to 30 % to compensate for data collection errors or nonresponses in the case of surveys.

3.3. Probability of Fixture Use

The probability of fixture use is the attribute we are interested in measuring from a population of various fixtures in CI buildings. There is expected to be a range of fixture p -values depending on the function of the CI building and the conditions of peak use experienced in the building.

3.3.1. Probability Calculation

The probability that a fixture is busy is the ratio of the duration of water flowing at a fixture to the total observation period. Omaghomi *et al.* (2020) analyzed water use data from over 1000 residential households collected during a two week period to estimate the peak hour fixture p -values. The peak hour was defined as the hour with the greatest volume of

household water consumption. The probability of use for individual fixtures was calculated using Eq. 3

$$p = \frac{\sum_k t_m}{\sum_k T} \quad (3)$$

where k is the number of identical fixtures, m is the number of water use events at a fixture, t is the flow duration during the peak hour, and T is the fixture observation window.

Depending on the type of CI building, the peak water demands can occur at any time, especially during peak use. For example, the peak window of water use in a sporting arena is expected during an intermission (*i.e.*, halftime), and there is usually a queue waiting to access the facilities. This queue scenario is not likely in an office building, restaurant, or hotel. The peak demand period first needs to be identified, and then the probability of fixture use calculated for that observation window.

Although measured data are paramount, there can be instances when measured information is unavailable, but observational data are accessible. Observing how fixtures are engaged in terms of the number of use events, volume, and duration of flow per fixture use event can be recorded. Such information can be utilized to estimate the peak period probability of flow at a fixture.

For the fixtures in a CI building, the probability of fixture use can be calculated based on observation and knowledge of the fixture flow characteristics. By monitoring the number of people gaining access to a fixture or group of fixtures (*i.e.*, restroom) in a building, the variables in Eq. 3 can be computed and the fixture p -value calculated.

The numerator in Eq. 3 is the total duration of flow from all water use events. This is the ratio of the flow volume (V) to the flow rate (q) at an individual fixture for all m water use events by the number of people arriving to use the fixtures or the number of people exiting the restroom (N) after using the fixtures and the percentage of people who activate the fixtures (a).

The duration of flow per pulse $t = \frac{V}{q}$ for a single water use event, while Eq. 4 is for all m water use events.

$$t_m = \frac{V}{q} Na \quad (4)$$

Similarly, the denominator in Eq. 3 is the total observation time for all k fixtures. That is a product of the number of fixtures and the observation window

$$\sum_k T = (k)(T) \quad (5)$$

Substituting Eqs. 4 and 5 into Eq. 3 and rearranging,

$$p = \left(\frac{N}{T}\right)\left(\frac{V}{q}\right)\left(\frac{1}{k}\right)a \quad (6)$$

Equation 6 simplifies to

$$p = \frac{\lambda\tau}{k}a \quad (7)$$

where λ is the departure rate calculated from the expression N/T and τ is the flow duration per pulse (V/q), and a is the fixture activation factor for k fixtures. Equation (7) is a variation of Equation (3), but expressed using terms that are relatively easy to monitor and measure during peak hour operation.

One noteworthy observation is that depending on the type of building occupancy, there might be a line waiting to access the facilities. This condition is referred to as congestion. The question is, how do the number of fixtures and the presence of congestion affect the probability of fixture use.

3.3.2. Simulation Exercise

The probability that a fixture is busy is based not only on the number of people having access to the fixture but also on the number of fixtures available. However, when the number of people exceeds the available fixtures and a queue is waiting to access the fixture, *i.e.*, congestion, the opportunity for fixture use is maximized. In theory, the probability that the fixture is busy is also maximized.

Adopting queueing principles to simulate arrivals and service at fixtures is one effective way to explore this phenomenon. Figure 3 illustrates our interpretation of service time in queueing theory to its application when simulating water demand at fixtures. In queueing theory, customers arrive at random according to a Poisson process and receive the service at a “server” (*i.e.*, the person or thing that provides the service, in this case, a fixture or an appliance) for a random length of time and then depart the system. The service time is when a server is engaged, that is, when a customer occupies the fixture. During the service time when a fixture is occupied, the customer draws water (*i.e.*, flushes the toilet, washes their hands, *etc.*). The duration of flow is needed to calculate the probability that an individual fixture will be busy in the water demand application.

Where there are k fixture “servers” in a restroom, the scenario can be described by the M/M/k or M/G/k queue process with a first in, first out queueing arrangement. M denotes an exponential probability distribution, while G is a general function.

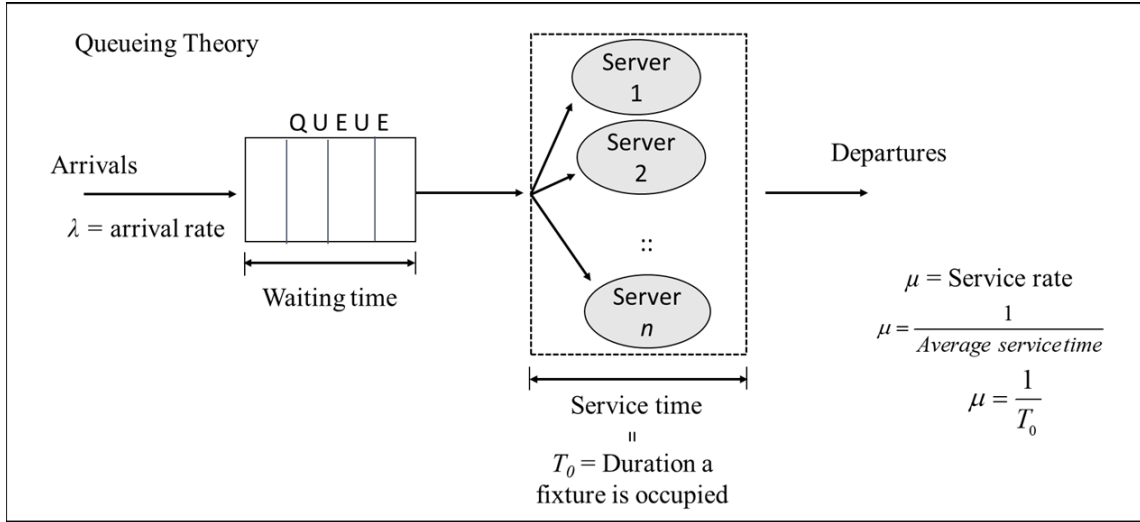


Fig. 3. Definition sketch for queuing theory applied to plumbing fixture use.

Server utilization is a dimensionless term that measures the system's performance. It provides a measure of the average use of the server (Gross and Harris, 1985). It is calculated as a ratio of the arrival rate to the service rate for k servers:

$$\rho = \frac{\lambda}{k\mu} \quad (8)$$

where λ is the arrival rate and μ is the service rate, and k is the number of fixtures “servers”. The service time and interarrival times are assumed to be independent and identically distributed. Arrivals at a restroom with k fixtures were simulated using the M/D/ k queue process. D denotes a deterministic service rate. Arrivals were assumed to be exponential, and the service time deterministic during which water is drawn at a flush valve toilet for 5 seconds. For this simulation exercise, the waiting time is infinite, and no customer is lost in the process. If a customer arrives and all the fixtures are occupied, the customer will wait in line for a service at the next available fixture. The fixture p -values and the utilization factor were calculated using Eqs. 3 and 8, respectively. Fixture activation was assumed to be 100 % ($a = 1$). Figure 4 shows the relationship between the probability of fixture use and the utilization factor for three service times, 60 s, 90 s, and 120 s. Each point is found as the average of 1 000 Monte Carlo simulations of the queuing process depicted in Figure 3.

At a utilization factor of 1, the arrival rate equals the service rate for all k fixtures, and the probability of fixture use is maximized. At this point, there is usually a queue (line of people) waiting to access the fixtures. Note that the utilization factor normalizes the number of available fixtures; hence the fixture p -value is the same even if the number of arrivals or fixture count in the restroom differs.

The greater the fixture occupation time, the less time the fixture is available to more users and the less probability of flow at a fixture, assuming a single flush per user. Similarly, the probability of flow at a fixture will increase or decrease if the duration of flow at the fixture increases or decreases, respectively.

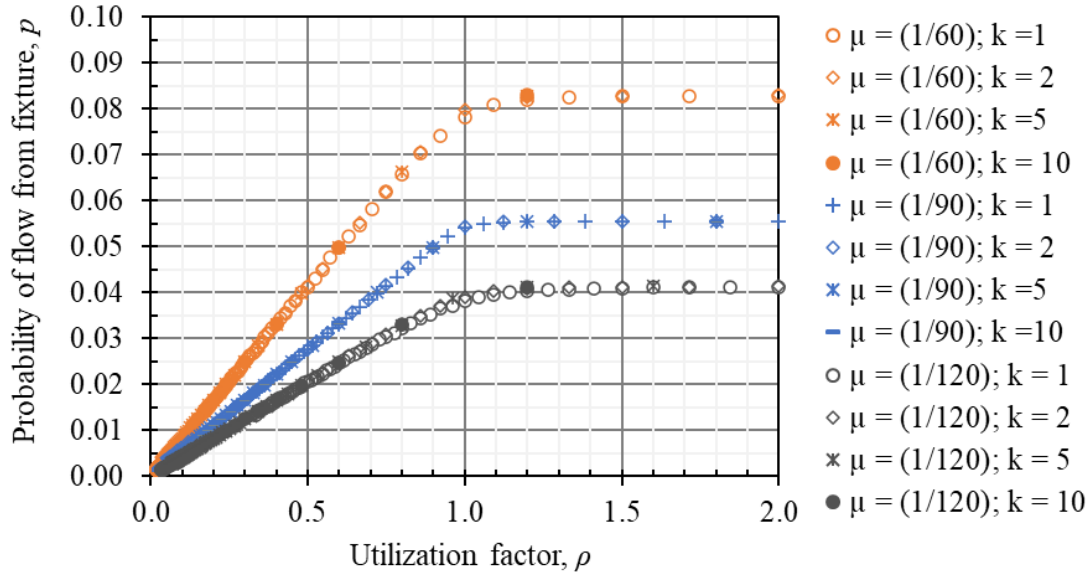


Fig. 4. Dimensionless $(p)||(\rho)$ diagram; probability plateau occurs at congestion.

This simulation exercise shows the relationship between the probability of flow at a fixture and fixture utilization in a restroom with multiple identical fixtures under congested use. A similar exercise can be conducted for fixtures in the various CI buildings. The results can be used to make estimates of fixture probability of use pending water use monitoring, data collection, and data analyses.

3.4. Sampling Methods

Various sampling strategies are broadly classified as either probability or non-probability sampling methods. Below are highlights of the different sampling methods.

3.4.1. Probability Sampling Methods

1. Simple random sampling: individuals are chosen by chance, and each has an equal probability of being selected. It allows for a calculated sampling error and reduces selection bias. Although it is a straightforward method, it may not select subjects with uncommon characteristics of interest.

2. Systematic sampling: individuals are selected at regular/specific intervals to ensure an adequate sample size. *i.e.*, for a sample size of n in x population, every x/n^{th} individual is sampled. This is more convenient than simple random sampling and easy to administer. However, if the sampling frame has been pre-ordered or has an underlying pattern, it may lead to bias.
3. Stratified sampling: here, the population is divided into subgroups with similar characteristics. This method is suitable for ensuring all subgroups' representation, and it improves accuracy and representativeness by reducing sampling bias. However, prior knowledge of the sampling frame is required to stratify by characteristics accurately.
4. Clustered sampling: here, the population is divided into subgroups known as clusters which are then randomly selected to be included in the study. This method is good for sampling over a wide geographical region. However, it might increase the risk of bias if the chosen cluster does not represent the population, thus increasing the sampling error.

3.4.2. Non-Probability Sampling Methods

1. Convenience sampling: this is the easiest sampling method, where participants are selected based on availability and willingness. Although useful results can be obtained, this sampling method is prone to volunteer bias, where the people who choose not to volunteer are different from those who volunteer.
2. Quota sampling: used mostly in marketing research, this sampling method specifies the number of each type of subject to be recruited. Ideally, the quotas chosen are proportional to the characteristics of the population and hence can be representative.
3. Purposive sampling: This is a subjective method of sampling where the researcher chooses a representative sample to suit the need of individuals with certain characteristics. For example, when media is sampling for public opinions. This method is prone to bias and will not necessarily be representative.
4. Snowball sampling: this method is common to social sciences, where existing subjects are asked to nominate/recruit other subjects known to know. This method is effective when a sampling frame is difficult to identify.

For this research, the stratified sampling method is the most suitable. Sampling for specific subgroups with similar characteristics, accuracy and representativeness can reduce sampling bias. In stratified sampling, water use fixtures will be sampled from subgroups based on the different types of CI buildings and their propensity for congestion during peak periods. For example, at one extreme, fixtures in public assembly buildings such as arenas and concert halls will most likely experience congestion during peak use, while fixtures found in offices, food service or lodging might experience peak use without congestion. At the other extreme, fixtures in religious or warehouse and storage buildings will only have

occasional use when the building is in use. Creating subgroups could reduce the categories of CI buildings and make it easier to implement in the Water Demand Calculator.

3.4.3. Example Sampling Plan

A hypothetical example is presented here to provide an idea of the density of the sensor network needed to monitor indoor water use at the fixture level. The leftmost column in Table 2 shows five CI building categories from Table 1: education, food sales/service, healthcare, lodging, office. These categories tend to have the largest annual water use per unit area among commercial buildings (Lewis 2017).

The column headings in Table 2 show seven fixture groups: water closet, lavatory, urinal, shower, dishwasher, clothes washer, kitchen sink. The 35 cells in Table 2 give the number of each type of individual fixture to be monitored, as computed using Equation (1) and based on the following five assumptions:

- [i] 95 % level of confidence ($\alpha = 5 \%$)
- [ii] 10 % margin of error
- [iii] representative fixture p -values, as given in parenthesis in Table 2
- [iv] the residence hall experiences congestion
- [v] one fixture per sensor

Based on the row sums in the rightmost column of Table 2, a total of 368 sensors are needed to monitor indoor water use at the five CI building categories. Some CI categories may require multiple buildings. For instance, if a single office building does not have 15 water closets, it will be necessary to add a second or third or more office buildings to reach the threshold of 15 monitored water closets. The amount of time each sensor remains deployed is an important consideration reserved for the phase 2 final report; preliminary analysis indicates the monitoring period will be two to four weeks for an individual fixture.

As noted in [v] above, the values in Table 2 assume “only” one fixture per sensor. It may be possible to strategically install a sensor on the premise plumbing so that it monitors more than one fixture. In this case, the total sensor count would be reduced.

Table 2: Hypothetical sampling plan for several categories of CI buildings.

Building Category	Sample Size: Number of Fixtures to Monitor / Sensors to Deploy (assumed p -value)							Total Sensors Needed
	Water Closet	Lavatory	Urinal	Shower	Dish Washer	Clothes Washer	Kitchen Sink	
Education (Residence Hall)	22 (0.06)	35 (0.10)	8 (0.02)	11 (0.03)	8 (0.02)	18 (0.05)	8 (0.02)	110
Food Sales and Food Service	4 (0.01)	8 (0.02)	4 (0.01)	0 (0.00)	8 (0.02)	8 (0.02)	18 (0.05)	50
Healthcare	8 (0.02)	11 (0.03)	4 (0.01)	15 (0.04)	4 (0.01)	22 (0.06)	11 (0.03)	75
Lodging	11 (0.03)	18 (0.05)	8 (0.02)	22 (0.06)	8 (0.02)	18 (0.04)	8 (0.04)	93
Office	15 (0.04)	11 (0.03)	8 (0.02)	2 (0.005)	2 (0.005)	0 (0.00)	2 (0.005)	40

4. Task 2: Wireless Sensor Network

4.1. Overall System

The objective of this research is to develop and test a novel, low-cost, battery-powered, miniature wireless sensor module for non-invasive detection of flow through pipes in premise plumbing systems (Fig. 5). When deployed in a typical commercial, industrial, or residential building, the modules will form a wireless sensor network to accurately monitor the incidence and patterns of water usage at various fixtures. Readings from this sensor network can be analyzed to estimate the peak hour p -values for various fixtures in the premise plumbing system, hence providing a sound basis to apply the promising new method for estimating peak indoor water demand.

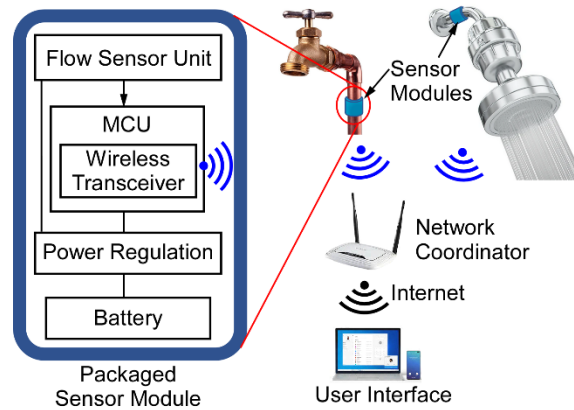


Fig. 5. System concept design.

Each sensor module in the wireless sensor network includes a non-invasive flow sensor unit, a microcontroller (MCU) with an embedded wireless transceiver, a replaceable battery, and a power regulation circuit (Fig. 5). The sensor modules will be connected to a central unit wirelessly, which will act as a gateway between the sensor network and the internet providing the users with remote access to the wireless sensor network.

4.2. Sensor Module Design

4.2.1. Overall Design of Sensor Module

The proposed design of each sensor module in the wireless sensor network is displayed in Fig. 6. The sensor module will include a non-invasive flow sensor unit, a microcontroller (MCU) with an embedded transceiver for wireless communication based on a low power protocol called Zigbee, and a replaceable battery along with the power regulation circuit. The flow sensor unit combines two sensor modalities. The acoustic measurement using a microphone is defined as sensor modality 1 (SM1), and the thermal detection based on heater and temperature readers is defined as sensor modality 2 (SM2). Both SM1 and SM2

will be implemented in the sensor module to form the hybrid detection to achieve both high accuracy and fast response time.

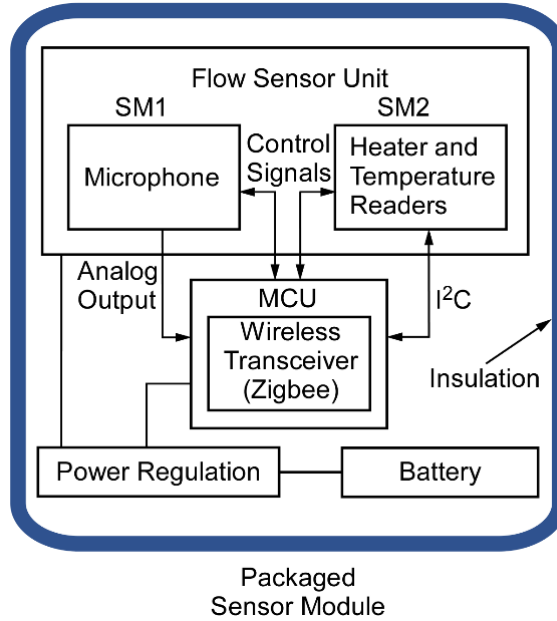


Fig. 6. Sensor module diagram.

The sensor module will operate in duty cycle mode, which means that it will stay in the sleep or standby mode for most of the time and only wake up to briefly perform periodic wireless communications or take measurements triggered by a water flow event. Considering all major power-consuming components with a duty cycle assumed for operation in either active, standby, or transmitting modes, the total average current or power was calculated. This value was used to estimate the lifetime of the sensor module powered by a high-capacity compact battery of 2.1 Ah capacity. The sensor module is estimated to operate with a lifetime of at least 39 days under the assumptions such as 50 measurements (or water flow events) per day, the average duration of water flow events of 4 min, usable battery capacity at 70 % of rated capacity, and others related to MCU energy modes. The actual lifetime will be evaluated after the device hardware and software are implemented. Further, the battery can be replaced with a different size or capacity, and if required, two or more batteries can be used together to provide an even longer lifetime.

4.2.2. Sensor Modality 1

4.2.2.1. SM1 Architecture

In the SM1, the acoustic detection will be done using a high-sensitivity miniature microphone chip, which will almost instantaneously detect the water flow on/off events.

We will be using a commercial MEMS microphone that has ultralow power consumption and a high signal-to-noise ratio (SNR) of 60.5 and has a size of only 3.76 mm x 2.95 mm x 1.3 mm. An important feature of this chip is that it can continuously monitor the surrounding sound in the sleep mode with low power consumption and send a triggering signal to wake up the MCU when the sound level exceeds a predefined threshold. Once awake, the MCU will record sound data from the microphone. An algorithm will process the recorded data. This algorithm includes signal filtering for the removal of noise and interference components. It also includes calculating a signal strength parameter to compare with a threshold that the experiments will determine. If the sound exceeds the pre-set threshold value, it indicates there is water flow, and MCU will turn on SM2; otherwise, the MCU and microphone will go back to sleep mode.

4.2.2.2. Figure of Merit for Detection Algorithm

The water flow detection algorithm comprises two parts, *i.e.*, the use of a digital filter and a function to calculate the signal strength indicator function. In developing the SM1 algorithm, a custom-defined Figure of Merit (FoM) is developed to quantitatively evaluate the effectiveness of different algorithms to differentiate between the water flow sound and noise. This is given as the detection algorithm output of water flow sound divided by the algorithm output of noise signals which can be a normal average or weighted average of different types of noises, as shown in the equation below. Higher FoM indicates a stronger capability of the algorithm to differentiate water flow sound from noise.

$$Figure\ of\ merit = \frac{R(Water\ flow)}{A_1R(Noise_1) + A_2R(Noise_2) + \dots + A_nR(Noise_n)}$$

where $R(Water\ flow/Noise)$ is an output of detection algorithm applied to water flow sound only or noise only, and $A_1, A_2 \dots A_n$ are weighting factors of different noise types.

For the signal strength indicator function, three candidates were considered which include RMS (power), energy, and amplitude. Table 3 defines and compares these three potential candidates, including a mathematical representation of each function.

Table 3. Comparison of candidate methods for signal strength indicator functions

RMS (Power)	Energy	Amplitude
1. Measures the power of a signal	1. Measure the energy of a signal	1. Measures the amplitude of a signal (sum of absolute values)
2. $R_{rms}(x) = \frac{1}{n} \sum_{k=1}^n x(n)_k^2$	2. $R_{eng}(x) = \sum_{n=0}^N x(n) ^2$	2. $R_{amp}(x) = \sum_{n=0}^N x(n) $

4.2.2.3. Algorithm Design and Evaluation

a) Selection of Filter

The digital filter will be used to remove the undesired noise signals while keeping the water flow sound in the recorded sound. The general criteria for selecting the filters for our application are as follows:

- i. Cutoff frequencies should be chosen to remove undesired frequency components of noise as much as possible (filters with steeper roll-off rates are preferred).
- ii. Less memory requirement (depends on type and order of the filter, lower order typically means lesser memory needed).
- iii. High computational efficiency (less computing power required).

Criteria ii and iii are important to allow the filter to be feasible for implementation with a microcontroller that has an ARM processor with limited memory size and computing capability. After carefully considering different filter classes, IIR filter class was selected because it is more suited for the application and should allow easier implementation.

IIR filter type consists of mainly 4 types of filters: Butterworth, Chebyshev type I, Elliptical, and Bessel. The elliptical filter is chosen as the initial choice for our application given its steepest roll-off between the passband and stopband of the filter spectrum. However, the elliptical filter is also the most complicated and difficult to implement given the limited computing power and memory size in the MCU. Further, Chebyshev (Type I) and Butterworth filters don't have as steep roll-off rates as an elliptical filter but are still acceptable and will be considered in further tests to evaluate their effects considering they are expected to be easier to implement in the MCU.

b) Determination of Filter Cutoff Frequencies

As the most important design parameter of filters, cutoff frequencies separate the passband and stopband. We evaluated the effect of cutoff frequency on the capability to differentiate between water flow sound and noises.

In this evaluation, FoM was calculated using normalized water flow sound and common noises while the filter cutoff frequency was swept for each signal strength indicator function. After evaluation, it was identified that the higher values of FoM lie between approximately 1.5 kHz to 3.2 kHz range which suggests that water flow sound dominates in that frequency range above the cutoff frequency compared to noise signals. However, the cutoff frequency will still be affected by the types of noises being considered. We considered 7 types of noises in this analysis and will consider other types for more thorough evaluations, particularly those recorded from realistic scenarios in the target deployment sites for field tests.

4.2.2.4. Preliminary Tests for Water Flow Detection

We performed preliminary tests of the selected algorithm on the capability to detect the water on/off events while some noises are in the background. These initial tests included 6 different

audio recordings, each with the water flow sound mixed with different noises (either one type of noise or a combination of different noises). These tests used an audio recording of water flow sound mixed with noises in a single audio file. The water flow signal had a flow rate of 4.0 L/min (1.05 gal/min) and noise signals had a typical sound level.

Table 4. Different audio recordings and their test results.

Recording	Noises	Water flow duration (sec)	Detection successful?
#1	Doctor office	3 to 8	Yes
#2	Music (soft beats)	3 to 8	Yes
#3	Hospital hallway	3 to 8	Yes
#4	Reception desk + Hospital hallway	1 to 6	Yes
#5	Patient room	2 to 7	Yes
#6	Patient room + music	2 to 7	Yes

Table 4 shows the different audio files used in these tests with various types of mixing of noises in the water flow sound and the test results. All audio recordings were successfully processed by the algorithm to detect correct on/off events. Further tests will be performed for algorithms in more scenarios and will also be evaluated with realistic data collected from field tests.

4.2.2.5. Preparation for Stage 1 of the Two-Stage Field Test

A two-stage field test has been planned to evaluate the sensor module under development. Stage 1 will be used to collect realistic sound data including both waterflow and noise for training and further testing the SM1 algorithm. Stage 2 will be used to test the whole sensor module and wireless sensor network. The following sections describe the preparation of a test device for the Stage 1 field test.

1. Device Configuration for Stage 1 Testing

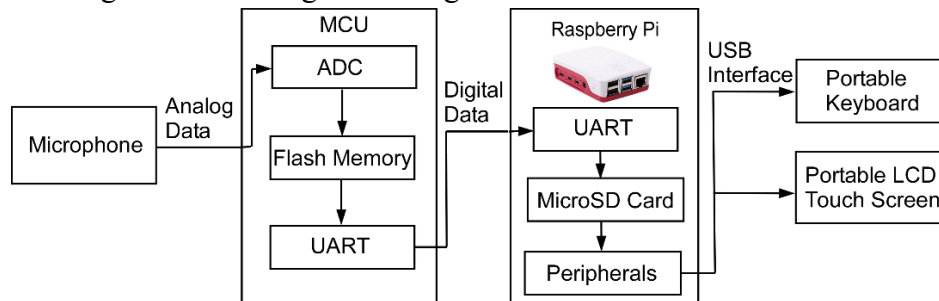


Fig. 7. Functional block diagram for device configuration for Stage 1 testing.

Figure 7 shows the configuration of the test device to be used for the Stage 1 field test. The test device includes a microphone, MCU, and Raspberry Pi, which is a credit card sized computer module. All these components are connected with wired connections. This test device will be mounted on a water pipe at the test site in the same way as planned for a real sensor module.

During the test, whenever there is a sound that exceeds the pre-set threshold, the microphone will wake up itself and also wake up the MCU to collect the sound data and activate the algorithm for processing the sound data. Otherwise, the microphone as well as the MCU will stay in sleep mode that has a negligible amount of power consumption to preserve battery lifetime. The sound data, which is in the form of analog sound signals will be sent from the microphone to the MCU and will be converted to digital data by analog to digital converter (ADC) of MCU. This digital data will then be stored on-chip in the flash memory which is a non-volatile flash memory. The data will be then communicated regularly through a wired communication to Raspberry Pi, which will be used to collect all the sensor data and store it into the MicroSD card inserted in this miniature-sized computer system. At the end of Stage 1 testing, all data will be retrieved from the MicroSD card for further training and testing of SM1 algorithms.

2. Stage 1 Test Printed Circuit Board (PCB)

The PCB that will be used in stage 1 testing has been designed, fabricated, and assembled. The size of this PCB is at 27.2 mm x 29.8 mm with 1.6 mm thickness, which can be further reduced easily by using smaller passive components and optimizing the layout further. This top side of the assembled PCB can be seen with all the components connected such as MCU, microphone chip, resistors and capacitors, switches and different connectors. On the back side you can see the acoustic port for microphone.

3. SM1 Microphone Integration

The acoustic port on the bottom of the microphone chip is aligned with a through hole on the fabricated PCB with a ring of solder. This is demonstrated in Fig. 8. The silicone coupling ring will be used to properly mount the PCB to the surface of the water pipe, forming an acoustic chamber which will help collect sound and enhance the acoustic coupling between the water pipe and the microphone chip while minimizing interference from the exterior noise. Another layer of insulation material will be wrapped outside the sensor module PCB to further reduce the noise interference while also providing thermal isolation for the SM2 thermal detection approach.

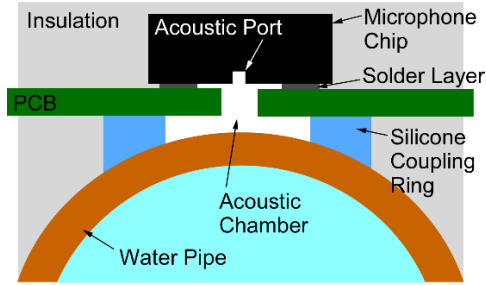


Fig. 8. SM1 microphone integration.

4. Stage 1 Test Setup

Figure 9 shows the photo of the Stage 1 field test system including all components. The figure displays the SM1 test PCB, Raspberry Pi with a transparent case and the size similar to a credit card, and a portable touch screen that can be used for field operation of the system for test initiation, etc. The portable keyboard can also be connected if necessary or just the touch screen can be used to do the control. A portable battery is also connected to power the test PCB and Raspberry Pi, as well as the touch screen and other components when they are used.

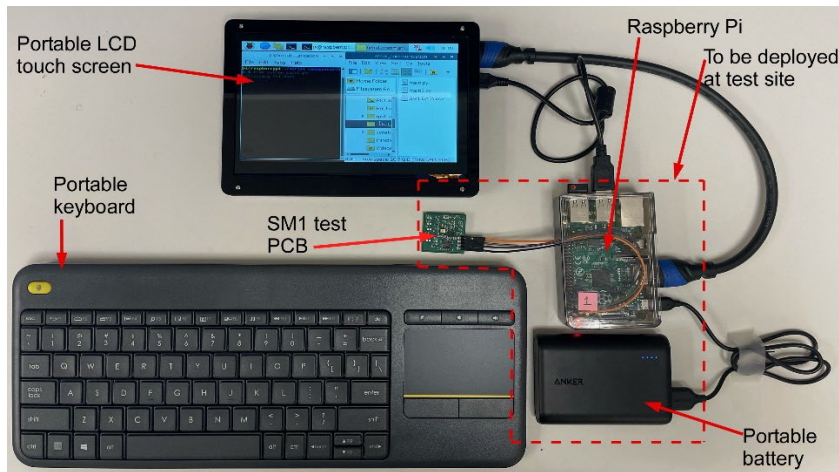


Fig. 9. Stage 1 test Setup.

The components inside red dashed line box will be the ones actually deployed and left at the test site by using adhesive tape or other means to secure to the water pipe. The image does not show the fiberglass insulation, which will be used to provide additional noise attenuation as necessary.

We performed initial overall system tests for the Stage 1 test device. Testing resulted in system lifetime of ≈ 33 hours. During these 33 hours, it was able to capture 4200 sound events resulting in 4.3 GB data collection (almost continuous recording of sound). The portable battery capacity used was 10 000 mAh. This system lifetime is less than our earlier estimation of 40 hours as lifetime can be heavily affected by the number of recorded events and can be extended using a larger battery. More in-house tests will be performed.

4.2.3. Sensor Modality 2

4.2.3.1. Detection Principle

Sensor modality 2 (SM2) is based on calorimetric thermal flow sensing method which is illustrated in Fig. 10. Two temperature sensors are placed symmetrically beside a heating element, one on the upstream side (T_1) and the other on the downstream side (T_2). When there is no flow, the temperature gradient created by the heater is symmetrical and the temperature sensors generate readouts $T_1=T_2$.

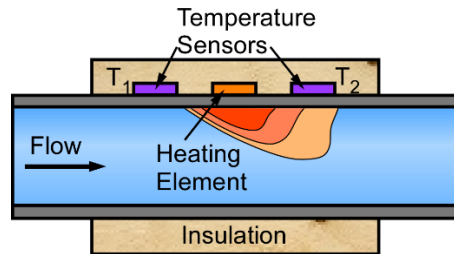


Fig. 10. Calorimetric thermal flow sensing method.

When there is flow, the temperature gradient is disturbed, causing $T_2 > T_1$. The temperature difference $\Delta T = T_2 - T_1 > 0$ indicates the presence of the flow, and its value correlates with flow rate. By using a heater and temperature sensors with a few mm size and embedding both on a small PCB, the thermal flow sensor can be made with a compact footprint to improve the detection sensitivity and reduce the power consumption. This thermal technique can potentially provide flow rate information although it will have a slower response time than SM1. Additionally, variations in pipe temperature readings with heater switched on during a water flow event may also be used as a feature for detecting water flow events or even more; we are in the process of investigating this method.

4.2.3.2. SM2 Design

For the SM2 test PCB, multiple designs have been considered with the temperature sensors placed at a distance of L from the heater. L will be varied in different designs of the PCB to evaluate its effect on flow detection. Multiple open slots are included around the temperature sensors to provide thermal isolation from rest of the PCB to help reduce thermal conductance. The symmetric placement of the upstream and downstream temperature sensors with respect to the heater is essential to minimize the offset in the readings from the two sensors. The center slot on the PCB will be used to align the heater centrally between the two temperature sensors. The fabricated PCB was assembled with all components (Fig. 11) using our in-house SMD reflow process.

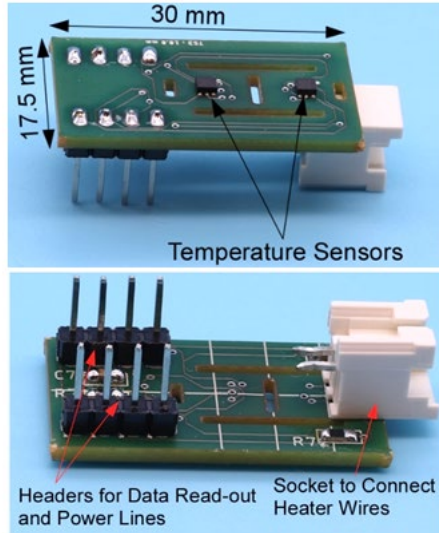


Fig. 11. Assembled PCB: top side (top), bottom side (bottom).

A high resistivity nichrome wire is used as the heating element. The nichrome wire is coiled around on a 3D printed heater holder to form the heater. The heater holder is designed to fit in the center slot of the PCB. An in-house precision wire winding machine has been built to precisely wind the nichrome wire on the heater holder.

4.2.3.3. Holder for Both SM2 Test PCB and Heater

When the heater holder was placed directly in the center slot on the SM2 test PCB as done in an initial design, heat could be transmitted directly from the heater coil through the test PCB to the temperature sensors according to results from extensive testing. Moreover, a better approach was required to place the test PCB and the heater on the water pipe for easier integration of the system on the water pipe. Considering these two aspects, we came up with a new two-part design of the holder (Fig. 12) for both the PCB and the heater, which can be manufactured using 3D printing and, if large volume production is required, through injection molding as well. Inside this holder, we have features to allow accurate placement of the test PCB on the holder and a bridge to be used as the heater holder. This bridge structure will have a place for the heater wire to be wound on and placed in the recesses on the holder without directly touching the test PCB, thus eliminating the direct heat conduction path from the heater coil to the temperature sensors.

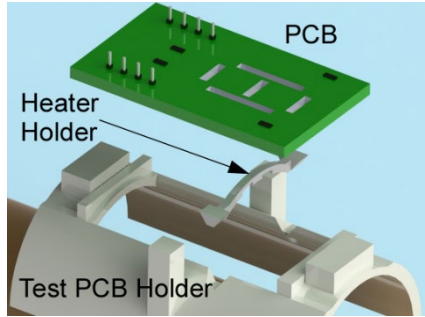


Fig. 12. Holder design.

The test PCB holder has a pair of recesses to allow the integration of the heater holder and four guideposts to allow the test PCB to sit accurately. Figure 13 shows the assembled SM2 test device after integrating the heater holder, test PCB, and test PCB holder. To print these parts, the on-campus 3D printing service was used.

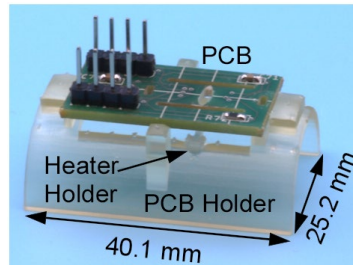


Fig. 13. Assembled test PCB for SM2 on PCB holder.

4.2.3.4. SM2 Test Setup

To facilitate the test of the SM2 thermal detection approach on water pipes of different materials and sizes, we developed a test setup that is compact to fit on our lab bench and easy to control water flow during the tests. The schematic diagram (Fig. 14 top) shows the design of the test setup, including both PEX pipes and copper pipes, each with sizes of 6.4 mm (1/4"), 9.5 mm (3/8"), 12.7 mm (1/2"), and 19.1 mm (3/4"). Two manifolds, one upstream and one downstream, are used to assemble all test pipes. Valves are included on each test pipe to allow individual control of the water flow. The test setup is connected to the water faucet in our lab through a digital inline flow meter that is used to monitor the flow rate and provide reference data for calibrating the optional flow rate measurement function of the SM2 sensor modality. Figure 14 bottom shows the implemented test setup. Compression fittings are used at all joints to allow reconfiguration of the test setup if it becomes necessary in the future. The test setup is assembled on a wood board and raised around the pipes using wood studs for operation convenience.

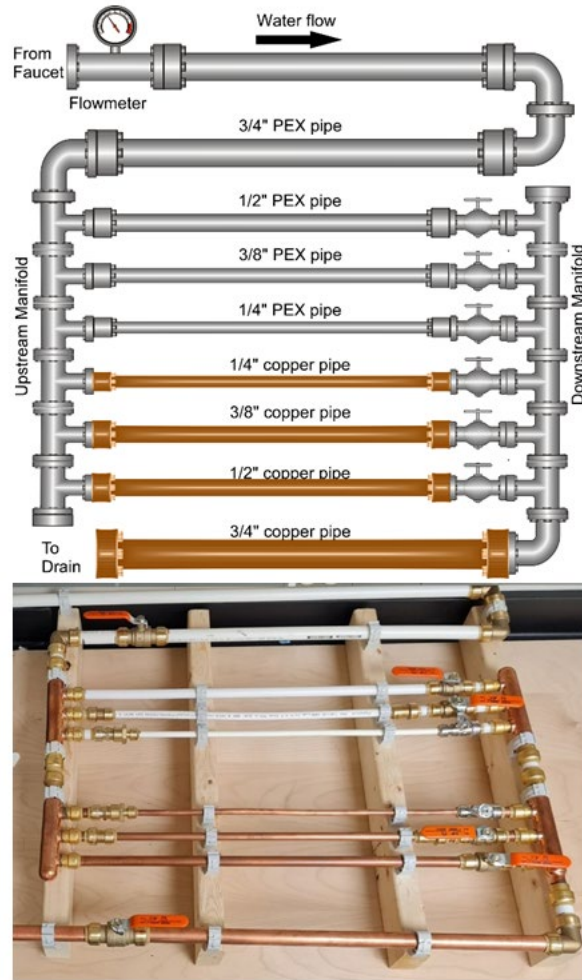


Fig. 14. Schematic of test setup design (top) and photo of implemented setup (bottom).

4.2.3.5. Initial SM2 Tests

The initial testing for SM2 was performed using the assembled PCB. The test setup used for the initial testing of SM2 is shown in Fig. 14. In these initial tests, the heater coil was manually wound into a small spherical shape and attached to the 19.1 mm ($\frac{3}{4}$ inch) water pipe directly using polyimide high-temperature tape. The temperature sensors on the assembled PCB were attached to the pipe such that the heater coil was located as close to the center point between the two temperature sensors as possible. A thermally conductive paste is applied on both the temperature sensors and the heater coil to transfer heat to the water pipe effectively. During the tests, the heater was turned on, and then the water flow was turned on and off repeatedly. Figure 15 shows the thermal response observed by the two temperature sensors during the tests. Figure 15 (top) graph shows the simple moving average (SMA) of the sensor readouts. The blue color represents the SMA downstream readout, whereas the green color shows the SMA upstream readouts. It is observed that the downstream sensor temperature increases more than the upstream readouts during the water flow on period, while during the water flow off period, the two temperature readouts

diminished, which agrees with the calorimetric detection principle. The same behavior repeated when we cycled the water flow on and off again. Figure 15 (bottom) graph shows the temperature difference between the downstream and upstream sensor readouts. When the water flow was on, the difference was higher compared to when the water flow was off. This test result successfully confirmed the water flow detection mechanism for the SM2 sensor modality.

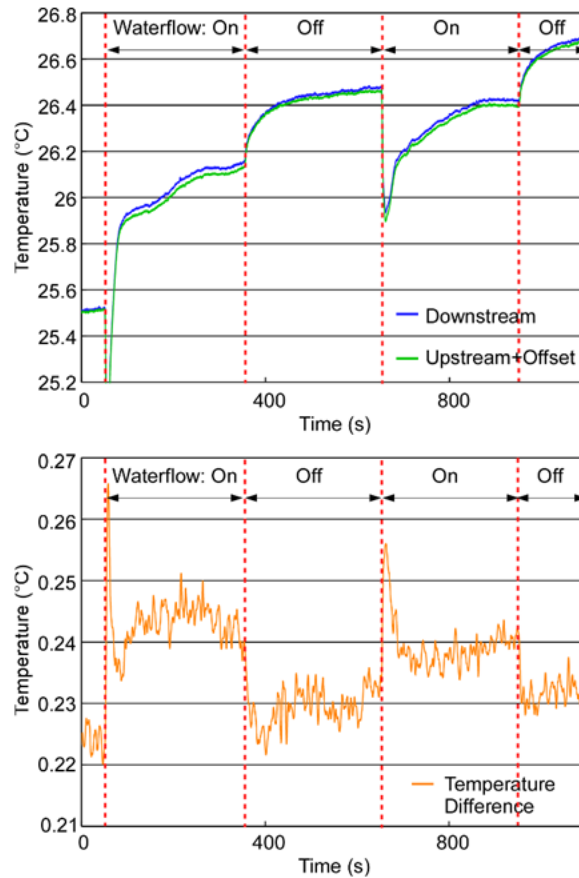


Fig. 15. Temperature response graph.

In the test results, an estimated offset correction had to be made in processing the data. Two types of offsets were observed: first, the inherent offset between the two sensor chips, and second, the offset due to the asymmetric placement of the heater with respect to the two temperature sensors. The inherent offset was corrected by calculating the average difference between the two sensors at room temperature. The offset due to the misalignment of the heater was corrected as much as possible using polynomial curve fitting. Further improvement of the PCB, PCB holder, and heater holder is necessary to minimize this offset and enhance the differential readout signal.

4.2.3.6. Investigation of Temperature Variation Profiles as a Potential Method for Water-On Event Detection

In tests performed with SM2 device that includes both temperature sensors and a heater, it has been observed that with the heater on and water flow on, the temperature profile recorded by the temperature sensor may provide a method for detection of water-on event with a faster response time than the differential thermal approach. To understand how temperature varies in water pipe with or without the heater under different environment conditions (outdoor weather, building temperature, etc.), extensive experiments are being performed on various scenarios that have been organized into five categories. We will implement the method for fast detection of the water-on event if a particular profile feature can be identified

4.3. Sensor Network Implementation

4.3.1. Overview

The wireless network for the distributed sensor system will be based on the Zigbee protocol, which is a low-power and low-cost wireless communication standard developed based on the IEEE 802.15.4 technical standard. Compared to low-power wireless technologies such as Bluetooth Low Energy (BLE), ZigBee can form a stable, reliable, scalable, and easily reconfigurable mesh network for battery-powered devices. Other advantages include a significantly larger limit on the number of nodes (up to a theoretical limit of 65 000), virtually unlimited range through data relaying, and wall penetration. The mesh network configuration also enables redundancy; data can be transmitted through an alternative route in case any node fails due to a drained battery or other malfunction.

4.3.2. Zigbee Wireless Network Configuration

Zigbee Wireless network (Fig. 16) will have a central unit that will act as a gateway to allow us to interface with the internet through Wi-Fi.

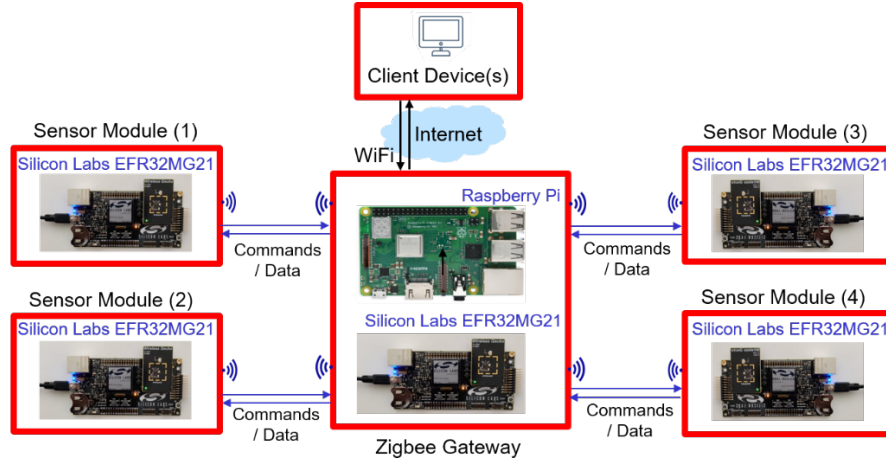


Fig. 16. Zigbee network topology.

This will give the users remote access from a laptop or smartphone to the gateway so that they can manage the sensor network and collect the recorded sensor data wirelessly through the Internet. The gateway will have two components, one is Raspberry Pi which is a credit-card-sized computer with built-in Wi-Fi capability, and the other is the microcontroller chip with a built-in Zigbee function to connect to sensor modules in the sensor network. For the implementation of the gateway, a circuit board with the microcontroller chip will be attached to the Raspberry Pi via the USB port. Each sensor module in the Zigbee network will receive commands and settings from the gateway and report sensor data to the gateway. A custom-defined data frame/structure will be used for the data report.

4.3.3. System Software Architecture

The software for the entire system is organized in 3 logical blocks, which follow the network hierarchy, comprising of the sensor modules, the wireless network gateway (based on the selected ZigBee protocol), and the remote computer / end-user device (Fig. 17). At the lowest level we have the sensor modules, which will be installed at various water monitoring locations. The sensor module consists of multiple functional blocks namely, SM1, SM2, ZigBee communications functions, data management and storage, and power management block. SM1 has an ADC operation and data processing block – to read and process the acoustic data from the microphone, and a water flow detection algorithm based on the acoustic data.

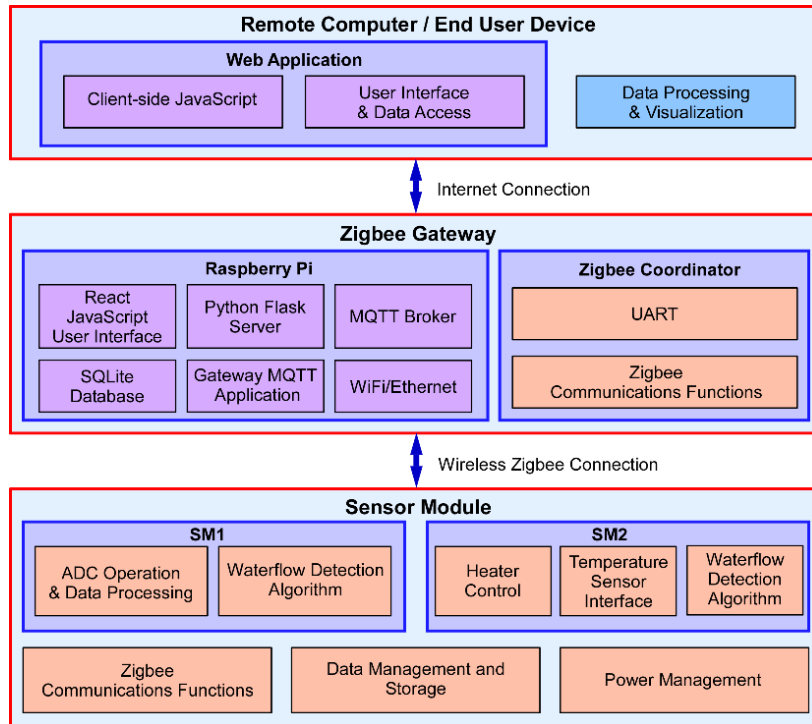


Fig. 17. System software architecture.

SM2 comprises of a heater control module - to control the on/off of the heater, a temperature sensor interface – to read data from the temperature sensors, and a water flow detection algorithm based on the thermal data. The sensor modules will be connected to the central unit wirelessly over ZigBee. The central unit in the middle acts as a gateway between the sensor modules and the internet. The gateway consists of a Raspberry Pi and a ZigBee coordinator. The ZigBee coordinator, which uses the same MCU as the sensor modules, has a ZigBee communication functions block – to communicate with the sensor modules wirelessly and ADC interface – to communicate with the Raspberry Pi. The Raspberry Pi has various blocks for serving the user interface webpage and interfaces the ZigBee network with the Internet through Wi-Fi or Ethernet connection. Finally, we have the remote computer at the top where the end-user will access the developed user interface through a web browser where the client-side Javascript will be running. Further data processing and visualization can be achieved by operating native applications on a remote computer.

4.3.4. Data Frame Definition

Figure 18 illustrates the definition of the data wirelessly transmitted from the sensor module to the Zigbee gateway. First, we have the Zigbee header, which is intrinsic Zigbee data that are necessary to start the data frame. Following the Zigbee header is the user data. The user data will include the results from both sensor modalities, including SM1 and SM2, where SM1 is acoustic, and SM2 is thermal. This includes the start and stop timestamps of the water flow event detected by SM1 (A and B). Next, we have the start and stop

timestamp detected by SM2 (C and D). After that, we have the temperature of the pipe and the temperature difference measured within the thermal flow sensor. Finally, we have an optional field for flow rate, which can be generated based on the results from SM1 or SM2.

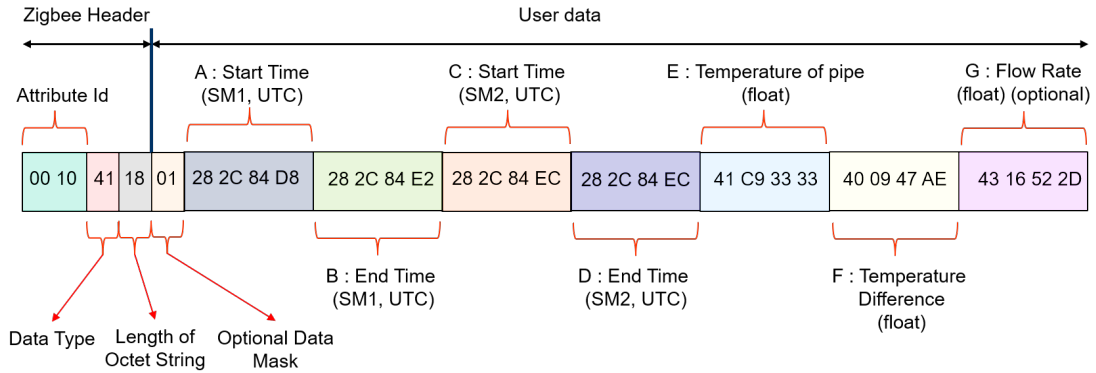


Fig. 18. Custom data frame used to report data from end device to gateway.

5. Task 3: Pressure Loss in PPS

The purpose of this task was to support NIST’s development of a plan to investigate pressure loss across fittings and other hydraulic appurtenances commonly found in modern premise plumbing systems. This task involves the overview of standard experimental methods to investigate hydraulic performance in premise plumbing systems.

As with Hunter’s curves published in the early 1940s, Clarke Freeman (1941) published a seminal research study on the pressure losses in pipe and fittings. Note, however, that the research was done by his father, John R. Freeman, in 1892. The measurements, conducted on a wide range of diameters and fittings common at the time, were mostly performed on steel pipes with threaded and flanged fittings. The results have been incorporated into plumbing codes and standard engineering reference tables and are still in use today.

However, steel pipe with threaded and flanged fittings is not commonly used in premise plumbing systems. Copper tubing with soldered fittings, cross-linked polyethylene (PEX) with insert fittings, polyvinyl chloride PVC with solvent cement fittings, and chlorinated polyvinyl chloride (CPVC) with solvent cement fittings are the most common materials used at present. Copper tubing with press fittings, stainless steel with press fittings, and polypropylene (PP) pipe with fusion-welded fittings are gaining market acceptance.

The internal roughness of modern pipe and fittings is very different from what Freeman studied in 1892. A comprehensive, independent assessment of the pressure losses for modern pipe fittings is long overdue.

Conceptually, the measurement of pressure loss is straightforward.

1. Establish a stable water pressure, which in turn enables stable flow rates.

2. Establish a temperature at which to run the experiments. If this cannot be maintained throughout the experiments, keep track of the actual temperatures during each test.
3. Determine the range of velocities at which to measure the pressure differential across a pipe segment with and without fittings.
4. Determine where to install the pressure gauges.
5. Determine the flow rates needed for each velocity, which are different for each internal pipe diameter.
6. Start the water flowing and record the pressure differential for a reasonable period of time.
7. Analyze the results.

In order to have data to assist with right-sizing premise plumbing systems, a member of our team began measuring the pressure loss in copper, CPVC, and PEX pipe and fittings in 2015, first at a lab in Southern California and later in Arcata, California (Fig 19, Fig 20).



Fig. 19. Pressure testing lab in Southern California.

Each pipe segment on a portable cart has 15.2 m (50 feet) of pipe, some with fittings and some without fittings. Pipe sizes range from 6.35 mm ($\frac{1}{4}$ inch) to 19.05 mm ($\frac{3}{4}$ inch) nominal.

The early tests determined the importance of having a very stable water pressure. The more stable the pressure, the easier it is to establish the target flow rate for each velocity. They also established the importance of having a relatively stable water temperature. In the Southern California lab, the water pressure varied more than 206.8 kPa (30 psi) over the course of only a few minutes, and the water temperature varied by more than 16.7 °C (30 °F) over the course of a day's testing: cold in the morning and much hotter in the afternoon.



Fig. 20. Pressure testing lab in Arcata, California.

Note the rectangular spiral CPVC test segment on the middle cart. The differential pressure gauge, temperature sensors, flow meter, and flow controls are on the cart in the foreground.

The lab in Arcata corrected these two issues. A large pressure tank was added to the testing system, which stabilized pressure, reducing the time to establish the target flow rates. And even without constructing tanks, chillers, and heaters to achieve a specific water temperature, the Arcata water supply temperature turned out to be very stable on any given day of testing. The Arcata lab also replaced two individual pressure sensors with a differential pressure gauge, eliminating the need to correlate the readings from different gauges. It was also decided to test pressure losses at 0.61, 1.22, 1.83, 2.43, 3.05 m/s (2, 4, 6, 8, 10 feet per second).

Target Flow Rates for 0.5 Inch Pipe					
Flow Velocity (ft/s)	2	4	6	8	10
	Flow Rate Target (gpm)				
0.5 inch PEX	1.10	2.21	3.31	4.42	5.52
0.5 inch CPVC	1.15	2.30	3.45	4.61	5.76
0.5 inch Copper	1.45	2.91	4.36	5.82	7.27

Fig. 21. Target flow rates for 1/2-inch nominal pipe.

The early results in Fig 21 showed very little loss in copper fittings compared to the values in the tables and compared to CPVC and PEX fittings. This highlighted the importance of ensuring that the signal-to-noise ratio (loss in fittings to loss in the pipe) was large enough to be observed by the test equipment. Recognizing the difficulties of accurately measuring the pressure loss of one fitting with the available equipment, the Arcata lab accounted for this by creating a test rig that had 4.8 m (16 feet) of pipe with and without fittings.

To ensure the ability to see the loss through copper fittings, there were ten fittings spaced more than 15 diameters apart so that there was no interference. The pressure and temperature measurements were made external to the pipe segments being tested. The difference between pipe with fittings and pipe without fittings created the total pressure differential. Divide the total by 10 to get the loss per fitting. However, the pressure loss in PEX insert fittings are much larger than through copper external fittings. Due to the constraints of the differential pressure gauge, which maxed out at 344.7 kPa (50 psi), it was sometimes necessary to reduce the number of PEX fittings.

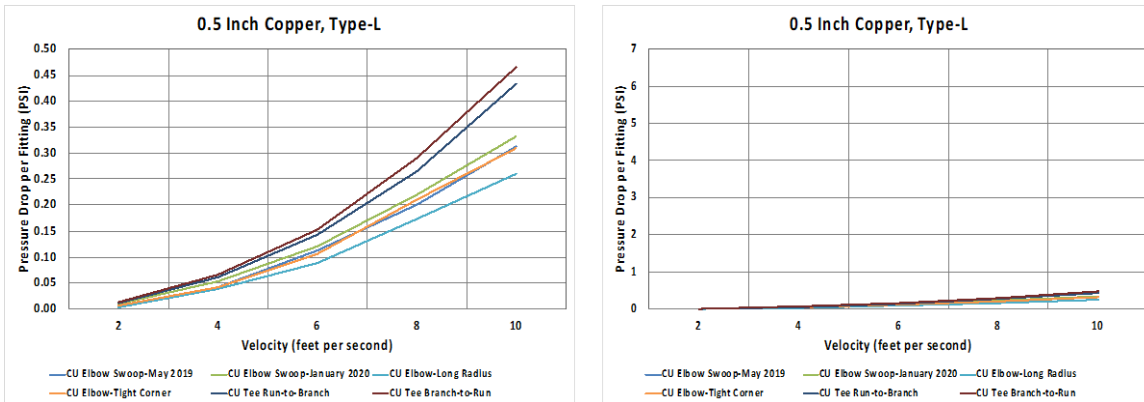


Fig. 22. Pressure loss through ½-inch copper elbows and tees.

Most fixtures and appliances in a home flow at less than 11.3 L/min (3 gpm), which is close to the target flow rate for 1.2 m/s (4 feet per second). At this velocity, the pressure loss is roughly 0.34 Pa (0.05 psi) per fitting. The graph on the right of Fig 22 has the same scale on the y-axis as the graphs in Figure 23, showing how small the pressure losses in copper fittings are compared to the losses in PEX fittings.

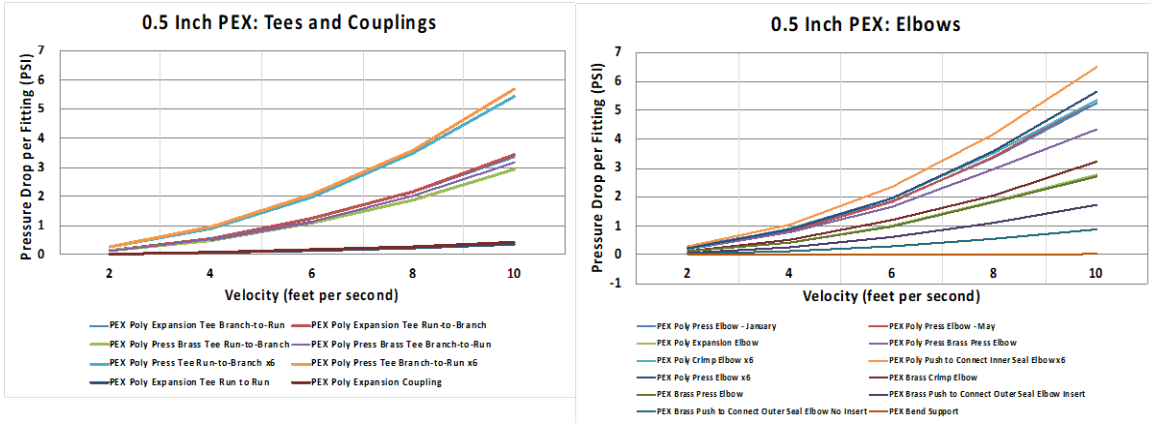


Fig. 23. Pressure loss through ½-inch PEX elbows, tees, and couplings.

To account for the same flow rates in a home, the velocity in PEX will be closer to 1.8 m/s (6 feet per second). At this velocity, the maximum pressure loss is about 13.8 kPa (2 psi) per fitting, roughly 40 times larger than copper.

Based on the results of these experiments, the UC team was able to advise the NIST team on how to best set up their experimental apparatus. The NIST test lab will be able to measure the pressure loss through one fitting, over a very wide range of pipe diameters, at specific water temperatures. These tests will enable the plumbing industry to have better data based on modern materials.

6. Summary and Recommendations

Although there are multiple categories of CI buildings, the sample size for the number of fixtures to be sampled will be calculated using a stratified method for subgroups depending on peak use conditions. In CI buildings where peak use occurs during congestion (*i.e.*, there is a queue), the fixture *p*-values are maximized. In contrast, other CI buildings that experience peak use without congestion will have lower fixture *p*-values. The simulation exercise showed that the fixture operational *p*-value is the same for restrooms with a varying number of fixtures having similar peak use conditions and utilization factors. Therefore, water use in any size of restroom can be monitored to identify the conditions of peak use and estimate their corresponding fixture *p*-value necessary to update the WDC for CI buildings.

The wireless sensor developed is a novel, low-cost, battery-powered, miniature wireless sensor module for non-invasive detection of flow through pipes. It works by detecting and confirming flow by any change in sound and temperature. The sensor with its acoustic and thermal modalities has been fabricated and is undergoing calibration testing. The acoustic measurement, SM1, listens for a change in sounds in the pipe that indicate flow. It can pick up other sounds around the sensor, such as people talking, footsteps, water flowing at other

fixtures, *etc.* The sensor has been calibrated to identify and filter out sounds that are not directly from the monitored pipe. The thermal modality SM2 acts as a validation to SM1. There are two thermal sensors upstream and downstream of a heater. A positive temperature differential between the downstream and upstream thermal sensor indicates flow. Both SM1 and SM2 work together in the hybrid detection of flow to achieve both high accuracy and a fast response time. Field testing of the sensor is currently underway at the Marian Spencer Hall at the University of Cincinnati to prepare data collection at various locations in the building and other CI buildings. The outputs from the sensor are recorded data with timestamps indicating when water is flowing. This data will be used to estimate the probability of flow at individual fixtures or groups of fixtures in a room.

The need to investigate the overall hydraulic system performance of a PPS cannot be overemphasized. The pipe size, choice of piping materials, and fittings impact the pressure loss in the pipes. The results expected from the experiments in the full-scale pressure-flow PPS lab will provide valuable insights into the relationship between reduced demand and its effect on pressure loss for various pipe sizes and materials.

7. References

- AWWA (in press) M22 Manual of Water Supply Practice: Sizing Water Service Lines and Meters, Fourth Edition, American Water Works Association, Denver, CO.
- Benazzi, R.B. et al. (1976), *“Water Requirements and Procedures for Estimating the Demand for Water in Buildings”*. CIBW62 Symposium
- Buchberger, S.G., E.M.J. Blokker, D.P. Cole (2012), *“Estimating Peak Water Demands in Hydraulic Systems I – Current Practice”*, in Proceeding of WDSA2012 Symposium, Adelaide, South Australia, Sept 24-27, 2012.
- Buchberger, S.G., T. Omaghome, T. Wolfe, J. Hewitt, D.P. Cole (2017) *“Peak Water Demand Study - Probability Estimates for Efficient Fixtures in Single and Multi-Family Residential Buildings”*, Executive Summary, IAPMO, Chicago, IL
- Cochran, W. G. (1977), *“Sampling techniques”* (3rd ed.). New York: John Wiley & Sons
- Cole, D.P. (2012) *“Determining fixture units for high-efficiency fixtures,” IAPMO.*
- Freeman, J. R. (1941), *“Experiments Upon the Flow of Water in Pipes and Pipe Fittings made at Nashua”*, New Hampshire, June 28 to October 22, 1982, Pranava Books, India.
- Gross, D., and C.M. Harris (1985). *“Fundamentals of Queueing Theory”*, 2nd Edition, John Wiley, New York, NY
- Herbert, K (2020) *“Gaining an Accurate Estimate of Water Demand in Buildings”*, Plumbing Engineer, 48(12):42-45.
- Hunter, R. B. (1940), *“Methods of Estimating Loads on Plumbing Systems”*. Rep. No. BMS65, US National Bureau of Standards, Washington DC.
- IAPMO (2018), *“Uniform Plumbing Code”*. IAPMO, Ontario, CA, Volume 1

Israel, G. D (2003), “*Determining Sample Size*”, Program Evaluation and Organizational Development, IFAS, University of Florida. PEOD-6. October.

Lewis K. (2017), “*Water Usage Data in the Commercial Usage Energy Building Survey*”, ASHRAE Winter Conference, Las Vegas, NV.

Omaghomi T., S.G. Buchberger, D. P. Cole, J. Hewitt and T. Wolfe (2020), “*Probability of Water Fixture Use during Peak Hour in Residential Buildings*”, ASCE Journal of Water Resources Planning and Management, 146(5).

[https://doi.org/10.1061/\(ASCE\)WR.1943-5452.0001207](https://doi.org/10.1061/(ASCE)WR.1943-5452.0001207)

Omaghomi, T., N.M. Ferretti, G. Klein, S.G. Buchberger (2022) “*Extending the Water Demand Calculator to Commercial and Institutional Buildings*”, ASPE Pipeline, June 15, 2022. https://www.aspe.org/pipeline/extending-the-water-demand-calculator-to-commercial-and-institutional-buildings/?_zs=2rlla&_zl=e88A3

Persily, A., D. Yashar, N.M. Ferretti, T. Ullah, W. Healy (2020) “*Measurement Science Research Needs for Premise Plumbing Systems*”, NIST Technical Note 2088, U.S. Department of Commerce, <https://doi.org/10.6028/NIST.TN.2088>.

Steele, A. (1982), “*Engineered Plumbing Design*”, 2nd edition, Construction industry Press, Elmhurst, Illinois, 267 pages.

USNCCIB (1974), “*Water Distribution and Supply within Buildings: National Research Needs, National Academy of Sciences*”, Counterpart Commission to CIB W-62.

US EIA CBECS (2020), “*Commercial buildings have gotten larger in the United States, with implications for energy*”, <https://www.eia.gov/todayinenergy/detail.php?id=46118> accessed Dec 12th, 2021

US EIA CBECS (2018), “*Building Types Definitions*”

<https://www.eia.gov/consumption/commercial/building-type-definitions.php> accessed Oct 28th, 2021.

Wistort, R. A. (1994), “*A new look at determining water demands in building: ASPE direct analytic method.*” Technical Proceedings; ASPE 1994 Convention, American Society of Plumbing Engineers, Kansas City, MO, 17-34.

Appendix A: Survey of plumbing industry at 2021 ASPE Technical Symposium

This section summarizes the presentation made at the 2021 ASPE Technical Symposium in San Diego on October 25th, 2021. The attendees were surveyed by the University of Cincinnati for their professional expertise and experience on the effect of low-flow, high-efficiency plumbing fixtures on indoor plumbing systems. A detailed review of the survey responses appears in the ASPE e-magazine *Pipeline* available at this link:

https://www.aspe.org/pipeline/extending-the-water-demand-calculator-to-commercial-and-institutional-buildings/?_zs=2rlla&_zl=e88A3

There were about 75 attendees in a standing-room-only presentation titled “Extending the Water Demand Calculator (WDC) to Commercial and Institutional Buildings”. The presentation covered the WDC, its current use, its future, and the benefits of adopting the WDC while showing examples that validate its predictions of peak water demand. Also discussed were the other research needs currently under investigation at the National Institute of Standards and Technology (NIST) related to reduced demand and pipe sizing, such as the relationship between pressure and low flow. There was a wide range of questions after the presentation that covered the capabilities of the WDC and the plans to extend its reach, the relevant research needs that should be reviewed alongside methods to estimate peak demand, and the possibility of adopting the WDC, especially in states that use the international plumbing code (IPC).

A 2-page written survey was conducted by the University of Cincinnati. Fifty-five attendees responded to the survey. Of all the responders, 98% identify as design engineers and some double as plumbing contractors and building engineers who install low flow and high-efficiency fixtures in residential and CI buildings. Due to the overestimation of peak demand for pipe sizing purposes, about one-third of the responders have changed their pipe sizing approach. The responders identified all parts of the premise plumbing system had been affected by the low flow fixtures, thus introducing poor performance of both the fixture and the system. The responders shared some ideas on research needs, such as investigating pressure loss for various pipe materials and fittings, updating pipe sizing requirements, and studying contaminants, pathogens, and biofilm formation in supply pipes. One of the areas repeatedly highlighted is the effect of low flow fixtures on wastewater drain lines.

Overall, the response to the survey was insightful and confirmed there is a research need to get fixture parameters for CI buildings and expand the use of the WDC.